Title: Dynamic model of basic oxygen steelmaking process based on multi-zone reaction kinetics: Modelling of decarburisation

Author 1 (corresponding author)
Name: Bapin Kumar Rout

Affiliation: Faculty of Science, Engineering and Technology, Swinburne University of Technology

Mailing Address: Hawthorn, Victoria, 3122, Australia, Email: brout@swin.edu.au

Phone: +61 3 9214 2837

Author 2
Name: Geoffrey Brooks

Affiliation: Faculty of Science, Engineering and Technology, Swinburne University of Technology

Mailing Address: Hawthorn, Victoria, 3122, Australia.

Phone: +61 3 9214 5672

Author 3
Name: M. Akbar Rhamdhani

Affiliation: Faculty of Science, Engineering and Technology, Swinburne University of Technology

Mailing Address: Hawthorn, Victoria, 3122, Australia.

Phone: +61 3 9214 8528

Author 4

Name: Zushu Li

Affiliation: WMG, University of Warwick

Mailing Address: WMG, University of Warwick, Coventry, CV4 7AL United Kingdom

Author 5

Name: Frank N. H. Schrama

Affiliation: Tata Steel, Netherlands

Mailing Address: Building 4H16, PO Box 10000,1970 CA IJmuiden, NL

Author 6

Name: Aart Overbosch

Affiliation: Tata Steel, Netherlands

Mailing Address: Building 4H16, PO Box 10000,1970 CA IJmuiden, NL

Abstract

In a previous study by the authors (Rout et al.[1]) a dynamic model for the BOF, employing the concept of multi-zone kinetics was developed. In the present work, the kinetics of decarburisation reaction is investigated. The jet impact and slag-metal emulsion zones were identified to be primary zones for carbon oxidation. The dynamic parameters in the rate equation of decarburisation such as residence time of metal drops in the emulsion, interfacial area evolution, initial size and the effect of surface active oxides have been included in the kinetic rate equation of the metal droplet. A modified mass transfer coefficient based on the ideal Langmuir adsorption equilibrium has been proposed to take into account the surface blockage effect of SiO_2 and P_2O_5 in slag on the decarburization kinetics of a metal droplet in the emulsion. Further a size distribution function has been included in the rate equation to evaluate the effect of droplet size on reaction kinetics. The mathematical simulation indicates that decarburization of the droplet in the emulsion is a strong function of the initial size and residence time. A modified droplet generation rate proposed previously by the authors has been used to estimate the total decarburization rate by slag-metal emulsion. The model prediction shows that about 76 pct of total carbon is removed by reactions in the emulsion, and the remaining is removed by reactions at the jet impact zone. The predicted bath carbon by the model has been found to be in good agreement with the industrially measured data.

Key words: BOF, decarburisation, slag-metal emulsion, droplets, multi-zone kinetics

1. Introduction

The refining reaction of carbon in a top blowing steelmaking process primarily takes place in the jet impact region and between metal drops and slag in the slag-metal gas emulsion. The total refining of carbon from the bath can be expressed as:

$$\left(\frac{dW_c}{dt}\right)_{total} = \left(\frac{dW_c}{dt}\right)_{em} + \left(\frac{dW_c}{dt}\right)_{iz} \quad (1)$$

55 Where $\left(\frac{dW_c}{dt}\right)_{total}$ is the total decarburization rate (kg/s), $\left(\frac{dW_c}{dt}\right)_{em}$ is the rate of carbon removal
56 from the emulsion zone (kg/s) and $\left(\frac{dW_c}{dt}\right)_{iz}$ is the rate of carbon removed from the jet impact
57 zone (kg/s).

58 The importance of slag-metal emulsion on the rate of decarburization reaction has been first
59 realized when the early researchers observed cavity and blow holes in the metal drops found
60 in the slag sample, collected from the upper part of the furnace.[2, 3] The significant low value
61 of carbon concentration measured in the metal drop compared to metal bath further indicates
62 that the ejected metal drops are decarburized to a large extent in the emulsion phase. [4, 5] The
63 emulsion mechanism of decarburization became evident when Mollseau and Fruehan
64 investigated the kinetics behaviour of Fe-C-S droplets in slag by using X-ray fluoroscopy. [6]
65 These authors observed that the metal drop containing carbon when it passes through high FeO
66 (>10 wt pct) in slag, it undergoes expansion in volume due to internal nucleation of CO
67 bubbles. The experimentally observed value of residence time of metal drop in the emulsion is
68 in the order of ~ 10 s, whereas the residence time of non-bloating dense drops accounts for
69 only a fraction of a second. [7] Considerably large volume expansion decreases the density of
70 drops and allows the decarburization reaction to proceed for a finite time in the slag-metal
71 emulsion phase. Large interfacial area for reaction caused by the breakup of the bulk metal into
72 small fragments along with ample reaction time (residence time) explains the rapid
73 decarburization kinetics observed in a top blowing steelmaking process.

74 Mathematical models have been developed to simulate the phenomena of bloating and
75 decarburization reaction kinetics of a single drop in slag.[7,8] The work resulted in the theory of
76 "bloated droplet" which subsequently applied by several authors to develop overall
77 decarburization model applicable for real converter process.[8-11] Different aspects of kinetic
78 models available in the literature for refining of carbon in the emulsion are summarized in

Table 1. The successful application of the theory of swelling of drops to an industrial scale decarburization model can be attributed to Dogan *et al.*[8] The authors applied the residence time model by Brooks *et al.*[12] and the droplet generation model suggested by Subagyo *et al.* [13] to calculate the overall decarburisation kinetics in slag-metal emulsion zone. The model used only mono-sized droplets and ignored the different modes of splashing on the kinetics of the process. In a recent study Rout *et al.*[14] proposed a correction in the previous droplet generation rate based on jet behaviour under high temperature environment and mode of splashing. Though Dogan *et al.*'s model provides a good explanation for the overall decarburisation rate, the model failed to explain the slow rate of decarburization kinetics during the initial blowing stage and unable to give explanation for the different decarburisation rate for different size drops. Also, the decarburization model by Dogan *et al.* overestimates carbon refining rate in the emulsion when the modified droplet generation was applied. **Figure 1** demonstrates the comparison of the carbon refining by the emulsion zone by Subagyo's model of droplet generation ($R_{B,T}$) with the one with modified formula suggested by Rout *et al.* In both the computation, the average size of the droplet was assumed 2.10^{-3} m. As can be seen from **Fig. 1**, in the case of modified droplet generation, the decarburisation rate predicted by Dogan's model is rapid and exceeds the measured decarburisation rate in the bath. The observed higher rate of decarburization rate is primarily due to a higher number of ejected metal drops predicted by the modified droplet generation correlation.

Several researchers reported that the size of a metal drop ejected from the melt exhibits a significant variation and the size spectrum can be mathematically described by Rosin-Rammler-Sperling (RRS) distribution function. [13, 15] Further, the examination of metal drops collected from the emulsion suggests that the kinetics of decarburization largely depend on the size of drops, the small sized drops. [2, 4, 5] Chen and Coley [18] observed that all the metal

droplets go through an incubation period before the swelling to take place. Those droplets which can be capable of nucleating CO bubbles before it falls back to the metal phase only increases the residence time in slag-metal emulsion. Since the rate of decarburization is proportional to the reaction time (residence time), the incubation time for CO nucleation plays a significant role in determining the refining rate of droplets. Further Chen *et al.* found that the incubation time is a strong function of C, S concentrations in the droplet and the level of FeO in slag.

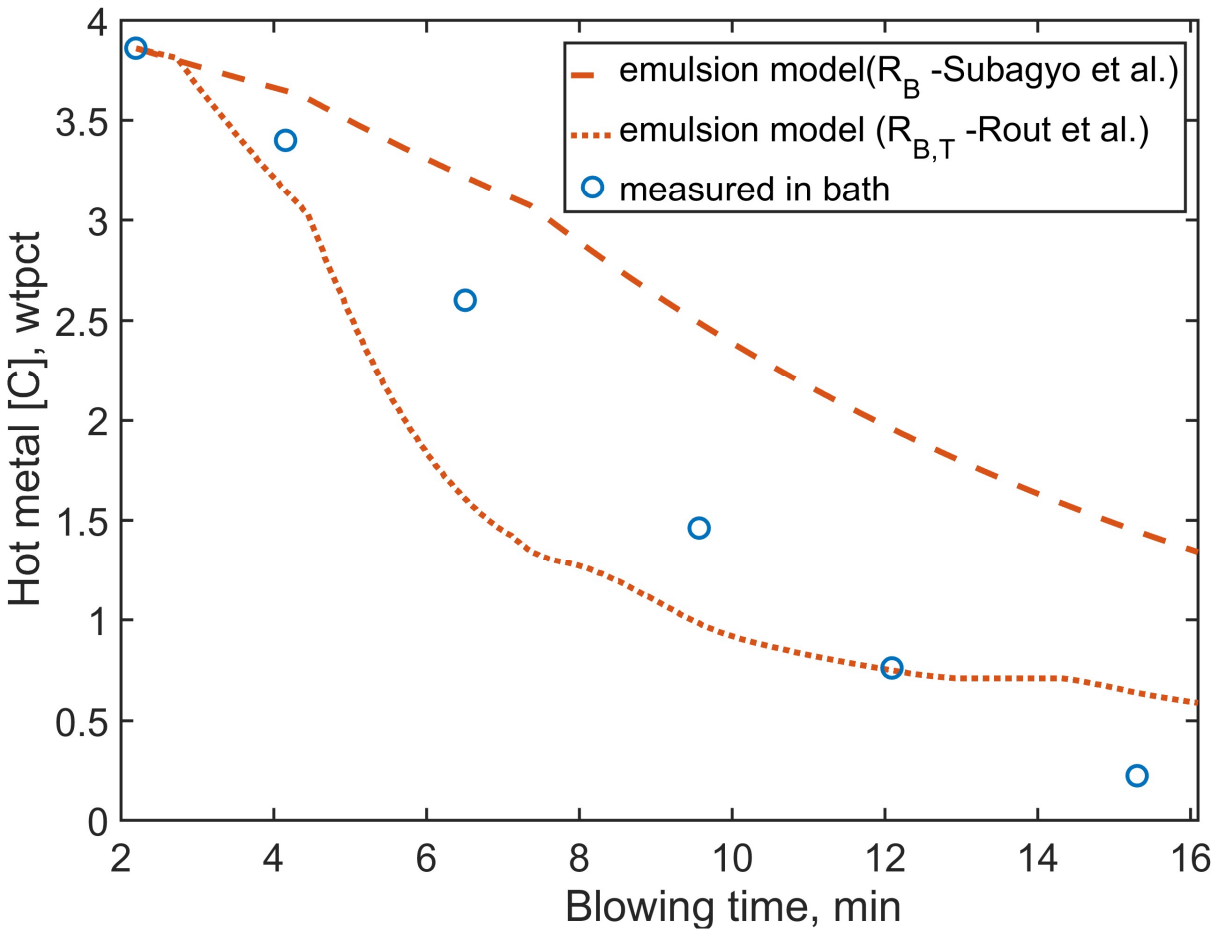

Figure 1: Dogan et al.'s model prediction of bath [wt pct C] refined by emulsion zone on the basis of different droplet generation rates

When a metal drop is ejected into the emulsion phase, other than carbon it contains several other impurities such as Si, Mn, P, S and it has been postulated that the removal of these impurities occurs simultaneously rather than sequentially. A recent study by Millman *et al.* [5] showed that thermodynamic equilibrium predictions might not be sufficient to explain the

118 refining path of these impurities. The apparent deviation from equilibrium thermodynamic
119 suggests that the process is controlled kinetically, and the simultaneous removal of C, Si, Mn
120 and P may be studied by a kinetically limiting approach. Several researchers reported that the
121 retardation of decarburization rate due to the presence of Si is associated with interfacial
122 phenomena, perhaps due to adsorption of SiO_2 at surface sites. [19-21] Mulholland *et al.* [19]
123 hypothesised that silica adsorbs into the surface sites and forms a thin layer of SiO_2 around the
124 drop which is responsible for inhibition of decarburization reaction. Woolley *et al* .[20] reported
125 that addition of Si and P decreases the decarburization rate by the formation of viscous oxide
126 layers at the slag-metal interface. Kim *et al.* [21] showed that the silica reduces the surface
127 tension of FeO-SiO_2 melts and can occupy up to 70 pct of the surface sites available for FeO
128 reduction reaction. Similarly, the firm surface active nature of P_2O_5 has been reported by
129 several researchers[2, 22] and the presence of P in the metal drop is responsible for retardation
130 of decarburization rate. Wei *et al.*[22] examined the effect of Si and P in the metal on
131 decarburization reaction and developed a kinetic model based on surface blockage effect of
132 oxides in slag. Sun *et al.*[17] reported that the presence of Si inhibits the decarburization rate of
133 the metal drop and the authors developed a kinetic model. Morales *et al.*[23] modified the
134 interfacial area by considering the surface active nature of SiO_2 to model the kinetics of FeO
135 reduction by carbon in an EAF (Electric Arc Furnace). However, the above models are limited
136 to only laboratory scale results and no attempt has been made to apply this surface limiting
137 approach for an industrial scale converter process.
138 The model developed in this study is an expansion of the framework of decarburization model
139 developed by Dogan *et al.* [8-10]. The present model is significantly improved by incorporating
140 several sub-models such as size distribution model to account for the size of drops, surface
141 coverage model and the modified droplet generation model. The effect of size and residence
142 time of the droplets on decarburization efficiency of metal drop in the slag-metal emulsion was

143 also investigated in the current study. The model predictions were compared with the measured
144 data of bath carbon in a 200 ton industrial converter.

145 **2. Model development**

146 The model for decarburisation is based on a multi-zone kinetics approach developed by the
147 authors in the earlier publication. [2] It has been observed that decarburisation in a BOF is
148 primarily led by the reactions in jet impact and emulsion zone. The refining of C in bath (in
149 bulk metal and slag-bulk metal) is significantly low in comparison to the above reaction
150 zones.[24] Therefore, in the present work, the BOF reactor has been divided into two distinctly
151 different regimes, i.e. slag-metal-gas emulsion zone and gas-metal reaction zone in order to
152 study the carbon refining kinetics. Decarburization rate in each zone has been computed
153 separately and finally combined by using mass balance equation. The concentration of carbon
154 in the bulk metal was calculated by the following mass balance equation:-

155

$$W_b^{t+\Delta t} \times [wt\ pct\ C_b]^{t+\Delta t} = W_b^t \times [wt\ pct\ C_b]^t - \left(\frac{dW_c}{dt}\right)_{em} \times \Delta t - \left(\frac{dW_c}{dt}\right)_{iz} \times \Delta t + \left(\frac{dW_c}{dt}\right)_{sc} \times \Delta t \quad (2)$$

156 Where W_b^t is the weight of the hot metal (kg) at time t, $W_b^{t+\Delta t}$ is the weight of the hot metal at
157 time step ($t + \Delta t$), pct C_b is the wt pct of C in the bulk, dW_C/dt is the decarburization rate
158 (kg/s) and the subscripts em, iz and sc correspond to emulsion, jet impact and scrap
159 respectively.

160 During the blowing process, the impurities like Si, Mn and P form their respective oxides and
161 join the slag phase, on the other hand, C forms gaseous product (CO and CO_2). Thus the
162 dynamic change in weight of the bulk metal has been calculated as:

163

$$W_b^{t+\Delta t} = W_b^t - \Delta W_m^{sl,t} + \Delta W_{sc}^{m,t} - W_m^{eject,t} + W_m^{return,t+\Delta t} \quad (3)$$

Here $W_b^{t+\Delta t}$ is the weight of the bulk metal at time t + Δt, W_b^t is the weight of the bulk metal at time step t, $\Delta W_m^{sl,t}$ is the weight of the metal forming the slag and $W_{sc}^{m,t}$ is the weight of the melted scrap during time step Δt. $W_m^{eject,t}$ is the weight of the metal droplets ejected at time t and $W_m^{return,t+\Delta t}$ is the weight of droplets return to the bath at time t + Δt.

2.1. Modelling of decarburization in the emulsion zone

The mechanism of bloated droplet theory has been used for estimating the rate of decarburization in slag-metal emulsion zone. The kinetics of decarburization for a single droplet in slag-metal emulsion can be described a simple first order rate equation in the following form [25]:

$$\frac{d[\text{wt pct C}]}{dt} = - k_d \frac{A_{app}}{V_{app}} \left([\text{wt pct C}] - [\text{wt pct C}]_{eq}\right) \quad (4)$$

Where [wt pct C] is the weight percentage of C in the droplet, $[\text{wt pct C}]_{eq}$ is the equilibrium C percentage at slag-droplet interface, A_{app} and V_{app} are the reaction area and volume of the droplet, k_d is the mass transfer coefficient.

2.1.1 Micro-kinetics: Decarburization of metal droplet in the emulsion

The "theory of bloating of droplets" was applied to evaluate the decarburization kinetics of metal droplets in the emulsion. .[12] Due to bloating (or swelling) of metal droplets in emulsion, the rate parameters are continuously changing during the reaction period. The mathematical treatment to estimate the key parameters such as residence time, droplet size, area and volume change associated with the droplets are already discussed in the earlier publication by the authors.[1] The mass transfer coefficient k_d was modified to take into account the surface coverage effect of oxides in the slag

A. Mass transfer coefficient

Brooks et al. [12] assumed carbon diffusion to be the rate determining step of overall decarburization of a droplet and employed Higbie's penetration theory to estimate the mass transfer coefficient. Since the ejected metal drops contain other impurities such as Si, Mn, and P,these elements, when exposed to oxidized slag, form their respective oxides at the vicinity of metal-slag interface. Some of the oxides (e.g. P_2O_5 and SiO_2) being surface active, lower the surface tension of the slag. Also, the presence of these components can physically block the interfaces or form a viscous layer (network forming oxides), which limits the surface area available for reaction. Ideal Langmuir isotherm can describe the fraction of unoccupied sites as:

$$1 - \sum\theta_c = \frac{1}{1 + \sum K_i a_i} \tag{5}$$

Here, θ_c is the fractional adsorbed sites covered by surface active oxides SiO_2 and P_2O_5, K_i is the adsorption coefficient of the i^{th} species and a_i is the activity of oxide.

For an ideal surface blockage model, the effective mass transfer coefficient for FeO-C reaction kinetics at metal drop-slag interface due to adsorption of SiO_2 and P_2O_5, can be described as:

$$k_{eff} = \frac{k_d}{1 + K_{SiO_2} a_{SiO_2} + K_{P_2O_5} a_{P_2O_5}} \tag{6}$$

The activity of SiO_2 and P_2O_5 have been calculated by the regular solution model. The adsorption coefficient K_{SiO_2} was calculated from the slope of the plot of surface tension of FeO-SiO_2 slag and logarithm of activity of SiO_2.[26] The detailed calculation of K_{SiO_2} has been illustrated in Appendix I. The value of $K_{Si\ _2}$was found to be 8.86 which is similar to the value reported by Wei *et al.*[21] The value of $K_{P_2O_5} a_{P_2O_5}$ has been taken from the relationship suggested by Hu *et al.* [27], which is equal to 0.65 (mole % P_2O_5). k_d is the mass transfer coefficient in the absence of surface active oxides, which was estimated by applying Higbie's

208 penetration theory. It should be noted that in the calculation of modified rate constant described
209 in Eq. 6, the effect of surface active element such as S and O in the hot metal are ignored. An
210 empirical correlation to incorporate the effect of S on mass transfer coefficient has been
211 suggested in the present calculation (see Appendix I). The authors acknowledge that due to
212 limited availability of experimental data, the effect of O on decarburization rate of metal droplet
213 has been neglected in the current work.

214 **B. Equilibrium [C] at slag-metal interface**

215 The reaction between FeO in the slag and C in the metal droplet at the interface can be written
216 as follows:

$$(FeO) + [C] = [Fe] + \{CO\} \tag{7}$$

217 Here it is assumed that the above reaction is at equilibrium at each calculation time step.
218 Accordingly, the dynamic equilibrium concentration of carbon has been calculated by

$$[wt\ pct\ C]_{eq} = \frac{P_{CO}}{a_{FeO} \times f_c \times K_c} \tag{8}$$

219 The partial pressure of CO gas was taken to be 1.51×10^5 Pa (average CO pressure inside the
220 vessel), activity of FeO (a_{FeO}) was calculated by applying regular solution model and activity
221 coefficient for carbon (f_c) was determined by an empirical correlation as a function of bath
222 carbon concentration. [28] Kc is the equilibrium constant which is a function of temperature and
223 derived from the standard equilibrium relation for carbon oxidation[29]:

$$\log(K_c) = 5.096 - \frac{5730}{T_m} \tag{9}$$

224 **2.1.2 Macro-kinetics: Total decarburization rate by emulsion**

225 The total decarburization rate by the emulsion phase, in a given computational cell, has been
226 estimated by calculating the difference between the mass of carbon ejected and the return of
227 carbon to the bath after refining :

$$\left.\frac{dW_c}{dt}\right|_{em}^{t} = \frac{W_c^{eject,t} - W_c^{return,t}}{\Delta t} \tag{10}$$

Where the total amount of carbon ejects into the slag-metal emulsion at time t, $W_c^{eject,t}$ was calculated from the information of droplet generation rate and the concentration of C in the bath as:

$$W_C^{eject,t} = \left(\sum_{p=1}^{P} \left(R_{B,T}\right)^{t}_{p} \times \Delta t\right) \times \frac{[wt\ pctC]^{t}_{hm}}{100} \tag{11}$$

P is the total number of divisions of the initial droplet size spectrum, $\left(R_{B,T}\right)^{t}_{p}$ is the rate of droplet generated (kg/s) for a given size range at time t and $[wt\ pct\ C]^{t}_{hm}$ is the concentration of carbon in the hot metal.

The micro-kinetics model estimates the final carbon concentration of the droplet at the time of its re-entry into the bath. At a given computation time, the total number of returning droplets having the final carbon concentration have been estimated and total weight of carbon entering to the bath was calculated.

$$W_C^{return,t} = \sum_{p=1}^{P} N^{return,t}_{p} \times \frac{[wt\ pct\ C]_{dp}^{return,t} \times w_{dp}^{return,t}}{100} \tag{12}$$

Here, $N_p^{return,t}$ is the number of returning metal drops, $[\%C]_{dp}^{return,t}$ and w_{dp} are the concentration of C and weight of the droplet just before its re-entry to the molten bath at a given blowing time.

2.1.3 Modelling of decarburization rate in jet impact zone

In the jet impact zone, decarburization takes place due to oxidation of carbon in the melt with gaseous oxygen and carbon dioxide at the gas-metal interface. Based on this mechanism, Dogan *et al.* [10] developed a mathematical model to estimate the total rate of decarburization in the impact zone. In the present work, the model proposed by Dogan *et al.*[10] has been applied to calculate the carbon removal rate $\left(\frac{dW_c}{dt}\right)_{iz}$ at each time step.

$$\left(\frac{dW_c}{dt}\right)_{iz} = \left(\frac{dW_c}{dt}\right)^{CO_2}{}_{iz} + \left(\frac{dW_c}{dt}\right)^{O_2}{}_{iz} \quad (13)$$

In case of decarburisation by CO_2, it was assumed that the rate is controlled by both mass transfer in gas phase and chemical reaction at the interface. The retracing effect of sulphur is also included in the kinetic model. The rate equation can be written as:

$$\left(\frac{dW_c}{dt}\right)^{CO_2}{}_{iz} = -100 \times M_C A_{iz} k_a P^b_{CO_2} \quad (14)$$

Where

$$k_a = \frac{1}{\frac{RT_f}{k_g} + \frac{1}{k_t}} \quad (15)$$

Here M_C is the molecular weight of C (g/mol). k_g, k_t and k_a are gas phase mass transfer coefficient, chemical reaction rate constant and apparent rate constant respectively. $P^b_{CO_2}$ is the partial pressure of CO_2 in gas phase, T_f is the interfacial temperature and R is the gas constant. T_f, the gas film temperature, is defined as the mean temperature between the bulk gas and the temperature at slag- metal interface. [10] The partial pressure of CO_2 was calculated from the molar rates of gas and the average partial pressure (P_{amb} =1.5 ×10^5 Pa) inside the converter. A dynamic post combustion ratio (PCR), as already discussed in the earlier work[1] was assumed to estimate the proportion of CO and CO_2 generated above the bath.

$$P^b_{CO2} = \left(\frac{N_{CO2}}{N_{CO2} + N_{CO} + N_{Ar/N_2} + N_{O_2}}\right) \times P_{amb} \quad (16)$$

Where N represents the molar rate of the respective gas species (CO, CO_2, O_2, Ar or N_2) and P_{amb} is the ambient pressure inside the furnace.

The rate of decarburisation caused by reaction with oxygen was assumed to be controlled by mass transfer in gas phase and can be expressed by the following equation:

$$\left(\frac{dW_c}{dt}\right)^{O_2}_{iz} = -200 \times M_C A_{iz} k_g (1 + P^b_{O_2}) \quad (17)$$

263 P^b_{O2} in the above equation was calculated by the similar method described in Eq. 16.

264 It was assumed that the rate of decarburization is controlled by mass transfer of C in the melt
265 when the bath carbon reaches a critical value. The critical value of C has been taken to be 0.3
266 wt pct.[28] The rate equation can be represented by first-order kinetics as:

$$\frac{dW_c}{dt} = -k_m A_{iz} \frac{\rho_m}{100} \times \left([wtpct\ C]_b - [wtpct\ C]_{eq}\right) \quad (18)$$

267 The jet impact area A_{iz} has been calculated assuming the shape of the area to be a paraboloid.
268 The mass transfer coefficient of the metal phase, k_m was estimated by the empirical
269 relationship as a function of stirring energy proposed by Kitamura *et al.*[30]

270 **2.1.4 Model formulation**

271 The mathematical framework, assumptions and the numerical calculation procedure for the
272 multi-zone reactions in a BOF has been discussed in detail in the earlier work.[1] In the case of
273 decarburization reaction, the sequence of calculation of overall refining rate obtained from jet
274 impact and slag-metal emulsion zone are illustrated in **Fig. 2.**

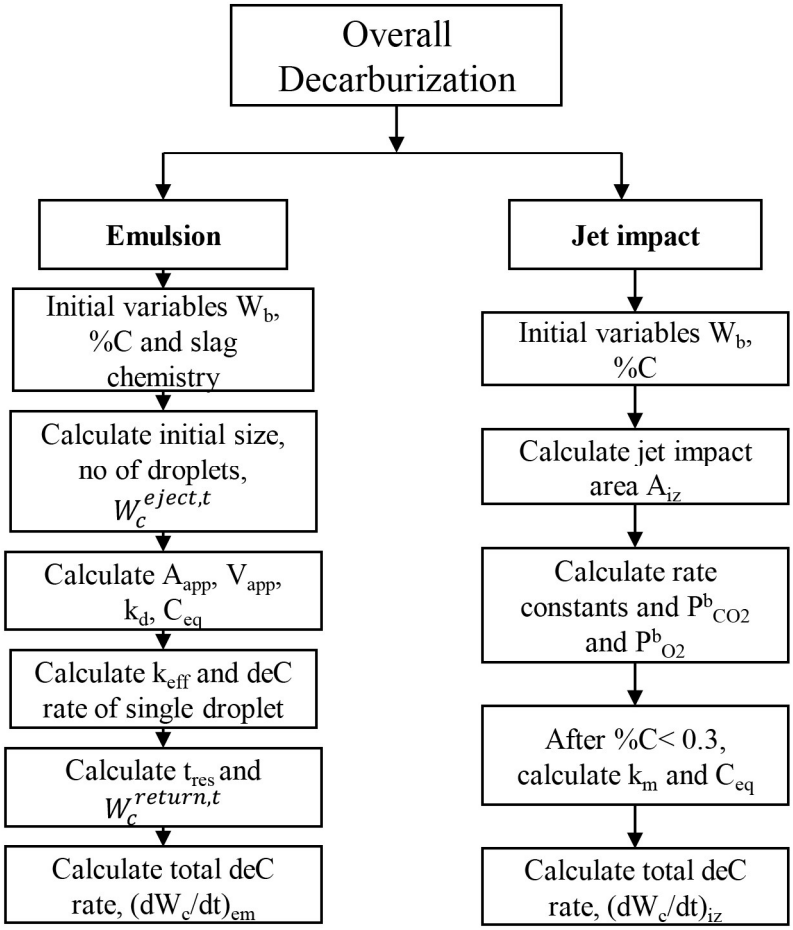

Figure 2: Algorithm for overall decarburization rate estimated from two reaction zones.

The slag generation model, simultaneously estimates the dynamic evolution of slag chemistry and used as an input to the decarburisation model at each numerical time step.[1] The various sub models like jet penetration area, droplet generation rate and residence time are connected in parallel to compute the transient change in the rate parameters for the evaluation of the decarburization rate in each zone..

3. Results and Discussions

3.1. Decarburization kinetics of Fe-C- Si droplet in slag

Molloseau and Fruehan[6] measured the decarburization rate of Fe-C-S droplet when it passes through FeO-CaO-SiO_2-MgO type slag. Considering that the decarburization kinetics follows first order rate equation, mass transfer coefficient was evaluated by fitting the measured C in

Eq. 4 by using least square approach. **Figure 3** shows the first order rate equation fitted with the experimentally measured data by Molloseau for 10 wt pct FeO in slag. The best-fitted value of mass transfer coefficient was found to be 0.002875 cm s^{-1} (R^2 = 0.97).

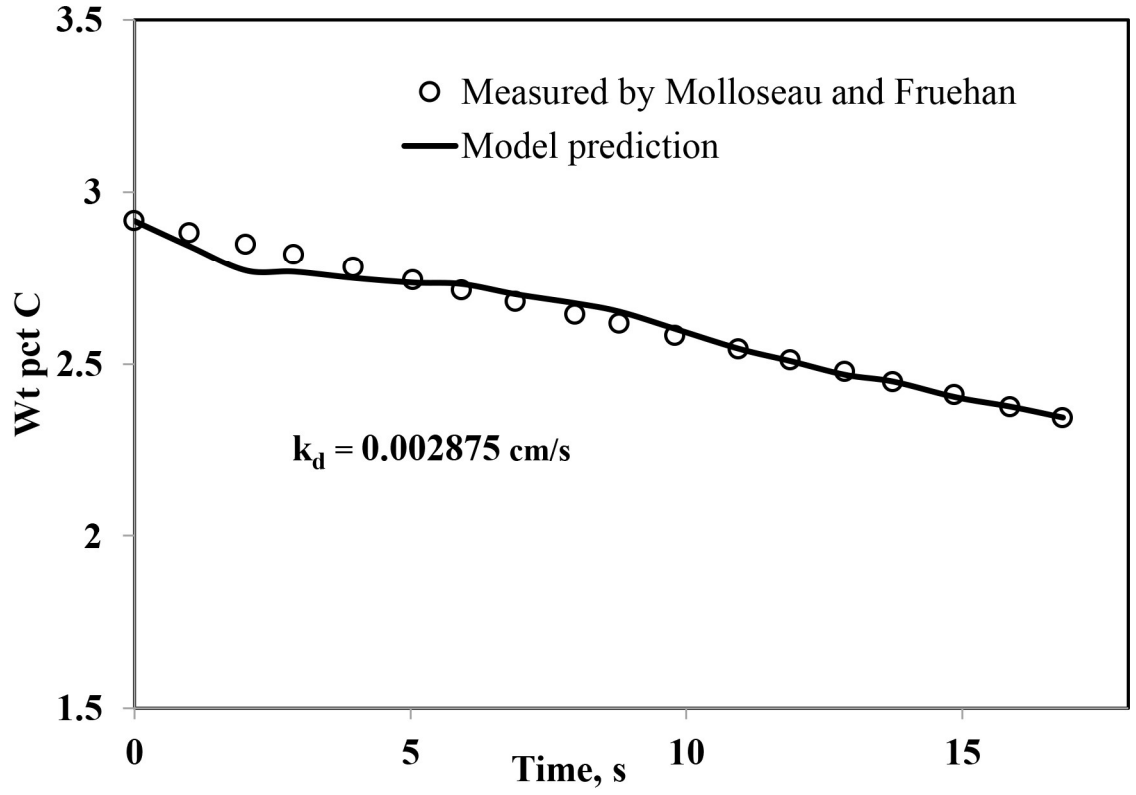

Figure 3: Estimation of mass transfer coefficient of C for Fe-C-S droplet

In another study by Sun *et al.*,[31] the kinetics of decarburization was measured for Fe-C-Si-Mn droplets in FeO-CaO-SiO_2-Al_2O_3 type slag. A comparative study has been performed to observe the effect of Si and Mn on the decarburization rate of the metal drop. **Figure 4** shows comparison between the rate of decarburization for Fe-C-S droplets with Fe-C-Si-Mn droplet reported by Sun *et al.* The solid line shows the model prediction of decarburisation with the mass transfer coefficient derived from the data by Molloseau *et al.* It was observed that the rate of decarburisation in the presence of Si slows down the decarburisation, a conclusion in agreement with several researchers.[19, 21, 31] In order to simulate the effect of Si on the decarburization rate, we have applied the surface coverage model due to SiO_2 in the slag and the effective mass transfer can be written as:

$$k_{eff} = \frac{k_d}{1 + 8.86 a_{SiO_2}} \quad (19)$$

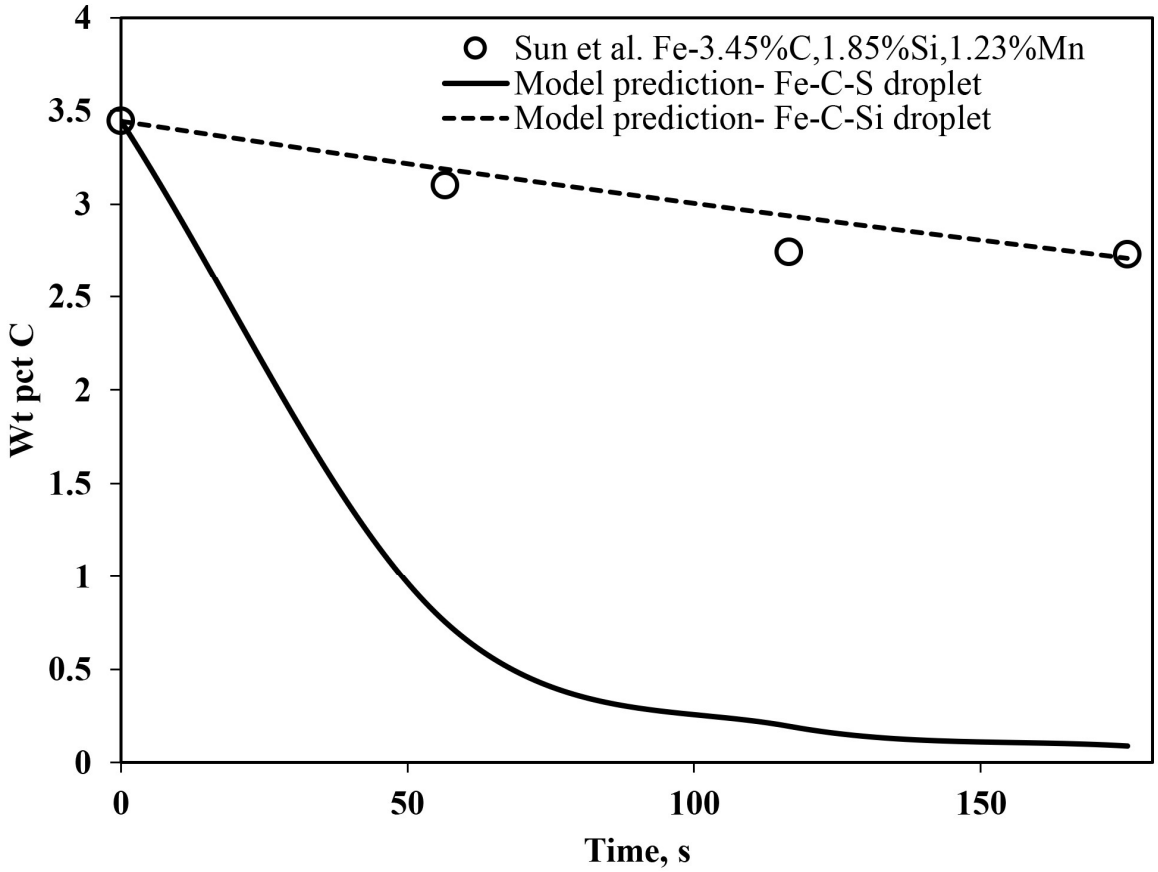

Figure 4: Modelling of decarburization kinetics of Fe-C-Si droplets in slag

The dotted line in **Fig. 4** is the predicted decarburization rate calculated by applying Eq. [19] at the slag-metal interface. As can be seen, an excellent agreement has been found between the model prediction and the measured value of carbon concentration, which shows that the observed slow decarburisation kinetics in the presence of high Si in the droplet can be explained by surface adsorption effect of SiO_2 described by the modified mass transfer coefficient by Eq. 18.

3.2. Decarburization efficiency of a metal droplet in emulsion

The following equation can express the decarburization efficiency of a metal droplet during a single metal circulation period (during the time of ejection from the melt to the time when it returns to the bulk metal):

$$\eta_c(\%) = \frac{C_{p,o}^{t} - C_{p,r}^{t+t_{res}}}{C_{p,o}^{t}} \times 100 \quad (20)$$

Where η_c is the efficiency of C removal for the droplet of size class p, $C_{p,o}^{t}$ and $C_{p,r}^{t+t_{res}}$ are the concentration of carbon (wt %) in the droplet at the time of ejection from the melt and the time of return to the bulk metal respectively.

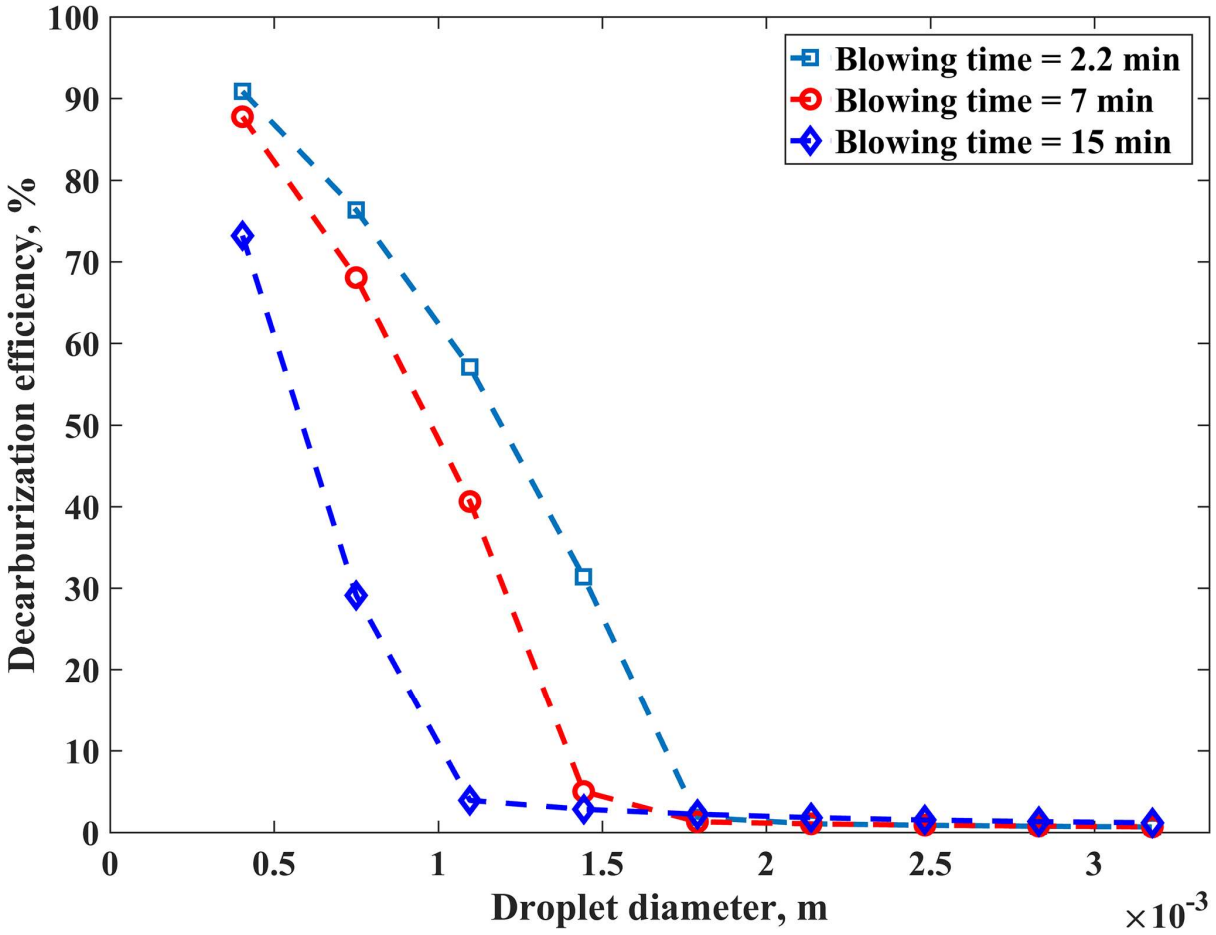

Figure 5: Decarburization efficiency of a metal droplet as a function of droplet size

Figure 5 shows the decarburization efficiency profile of the metal droplets as a function of its diameter during the different blowing periods of blowing. As can be seen from the figure, the droplets in the lower region of the size spectrum exhibit a higher value of efficiency as compared to the bigger droplets. A similar observation has been reported by Millman *et al.*, suggesting that the small sized droplets decarburise strongly as compared to the larger sized

326 droplets. [5] By examining the metal samples in the emulsion collected from a real converter,
327 Cicutti *et al.* [4] also reported that the decarburization efficiency of a metal drop is a strong
328 function of the size of droplets. The smaller sized droplets (≤ 0.0005 m) can achieve more than
329 80 pct of carbon refining by emulsion. A similar observation was maded by Millman *et al.*[5]
330 in a 6-tonne pilot scale converter. It was observed that apart from strong decarburization, the
331 concentration of other elements such as P, Mn, and V are extremely low for a droplet of the
332 size of the order 0.1 mm (~ 10^{-4} m). The numerical predictions obtained from the present work
333 also find similar observations. For droplets having an initial size of 0.4 mm (4×10^{-4} m), the
334 efficiency decarburization was observed to be as high as 90 pct. As the size of metal drops
335 increases the refining efficiency gradually decreases. Accordingly, the model predicts that in
336 order to achieve high decarburization efficiency, the initial size of the ejected droplets should
337 not exceed a certain order of magnitude. This behaviour can be explained by analysing the
338 residence time of the metal drops in the emulsion phase

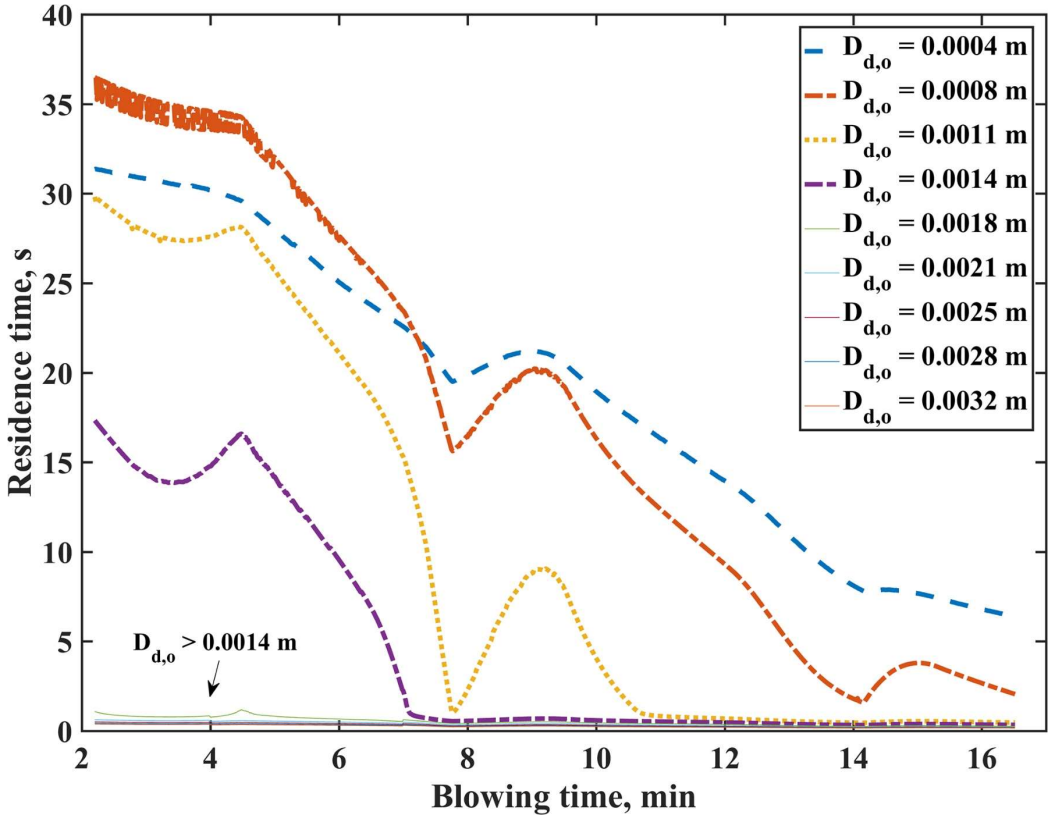

Figure 6: Residence time prediction of the metal droplets in slag as a function of blowing time

The residence time of a droplet in the slag-metal emulsion can be related to the ability of metal droplet to remain buoyant. Dogan *et al.*[9] reported that the residence time of the metal droplets having high carbon concentration exhibits longer residence time in the emuslion regardless of their initial size. This conclusion can be true for Fe-C droplets. However, in the presence of Si, Mn and P in the metal, the rate of CO nucleation inside the drop either delays or decreases and can certainly affect the droplet swelling process. **Figure 6** shows the calculated residence time of a Fe-C-Si-Mn-P metal droplet by applying the surface blockage model. It is interesting to observe that the residence time of the droplets increases with increase in the diameter of the droplet to a certain size and then decreases during the initial part of the blow. However, the droplets in the lower size spectrum exhibit long residence time compared to larger sized ones during the second stage of blow (~ after 7 minutes). Further, it was observed that the ejected droplets whose mean diameter is more than 1.4 mm (1.4×10^{-3} m) are incapable of bloating and

thus return to the bath immediately, which results in significant reduction of carbon refining in the molten metal. Figure 6 shows the predicted residence time as a function of the blowing time, which is a complex function of lance height, slag FeO, C concentration and decarburisation rate in the bulk metal. A sudden change in the predicted residence time profile at 4^{th} min and 7^{th} minutes is primarily caused by change in lance height during the blowing operation.

The residence time behaviour of the metal droplets for small droplets can be explained qualitatively by analysing the mechanism of swelling of droplets in the slag-metal emulsion. Chen and Coley [18] shows that swelling will only occur if CO bubble nucleates before the metal droplets return back to the metal phase. The study indicated that the total time of flight (ascending-bloating-descending) of the dense droplets should be more than the incubation time for nucleation of CO gas, which is illustrated in **Fig. 7**. The incubation time for bloating is a strong function of carbon concentration and FeO in slag, and it sharply increases with the decrease in carbon concentration. The competition between incubation time for CO nucleation and time of flight of the dense droplet decides whether the bloating (or swelling) will occur or not.

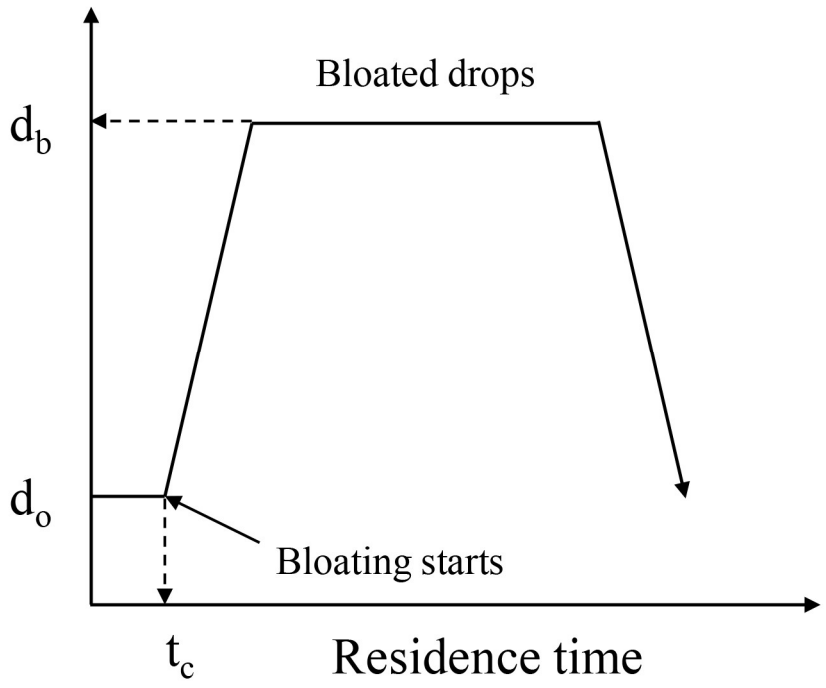

370

371 Figure 7: Qualitative representation of the mechanism of bloating of metal drops in slag

3.3. In line with the experimental evidence by Molloseau *et al.*,[5] modeling results by Brooks *et al.*[7] and Dogan *et al.*[9] suggested that large drops exhibit long residence time due to the presence of high carbon concentration. However, these observations are based on Fe-C-S metal drops, and theretarding effect of Si, Mn and P on bloating process was not considered. As reported by Sun *et al.*,[17] in the presence of Si, Mn and P in the melt, the decarburization kinetics reduces significantly. The nucleation of CO bubblesbecomes easier for small sized droplets having high carbon and slag containing high concentration of FeO. It may be due to the large value of surface area to volume ratio (A_{app}/V_{app}) and mass transfer coefficient associated with small sized drops (k_d α $1/d_{drop}$) that enhances the decarburization rate to reach the threshold level for bloating in a quick period of time. . Once theese droplets become buoyant in emulsion, the remaining carbon can facilitate the nucleation process and hence can increase the residence time. This behaviour can be seen from Fig. 6, where the residence time is predicted to be reach a maximum value for 0.8 mm (8×10^{-4} m) diameter droplets during initial blowing period (< 7 min). After approximately 7 min of the blow, the lower sized droplets were observed to exhibit high residence time in slag. Large drops having diameter more than 1.4 mm (1.4×10^{-3} m), on the other hand, spends only a fraction of second in the emulsion. The reason for this small residence time may be due to slow rate of decarburization associated with the large diameter drops that failed to achieve the threshold decarburization for the initiation of bloating process during the flight time in the emulsion.Decarburization rate in emulsion

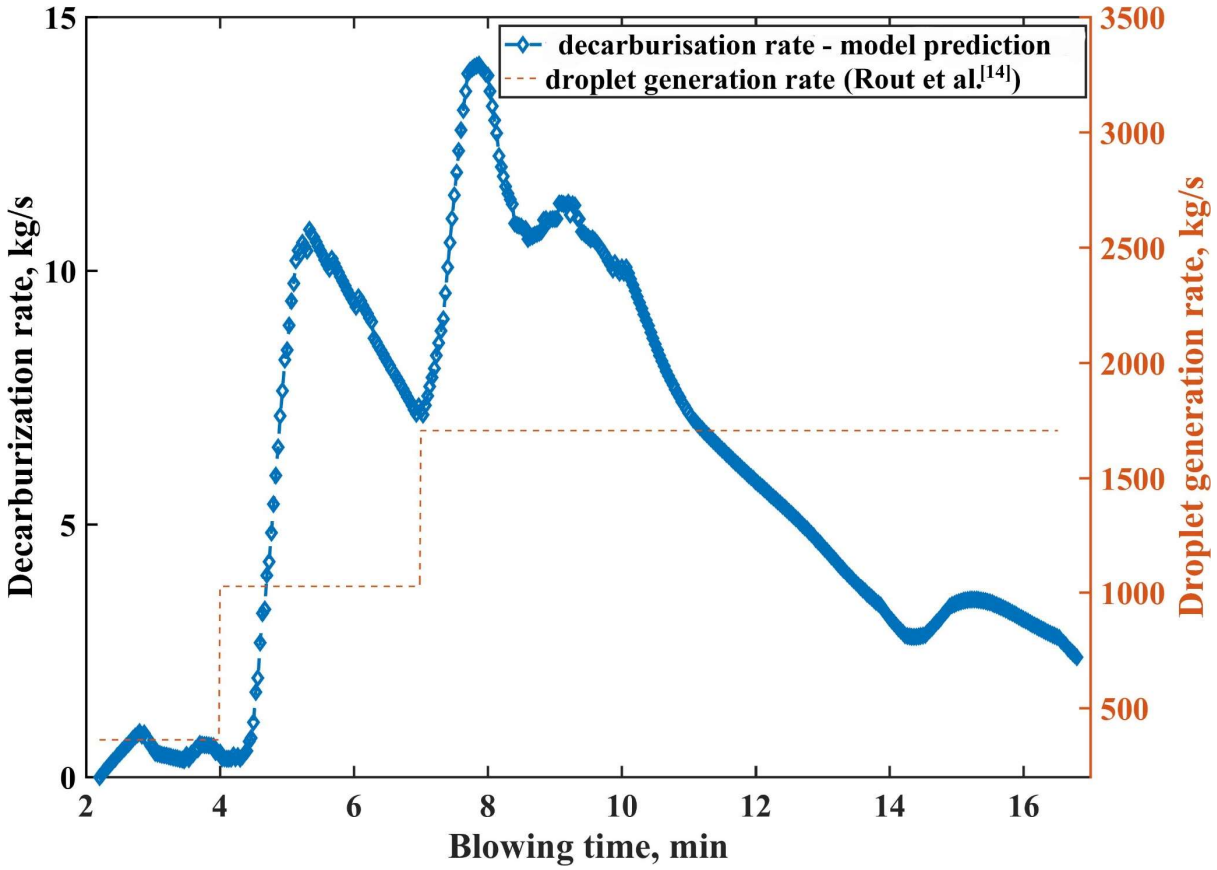

Figure 8: Decarburization rate by emulsion calculated by the model

Overall decarburisation rate in the emulsion zone was computed by combining the carbon refining from all the metal droplets in the emulsion at each computational time step. **Figure 8** shows the overall carbon refining in the metal droplets in the slag metal zone as a function of blowing time. It was observed that during the initial part of the blow (< 4.5 min), the overall refining rate of carbon due to the slag-metal emulsion is considerably low, i.e. the predicted decarburization rate falls below 1 kg/s. The low rate of decarburization can be explained by the amount of droplets present in the emulsion and the kinetics of reaction during the initial part of the blowing process. During the first minutes of the process, the lance height is kept at a higher position which leads to less number of metal droplets ejected into the emulsion. Also, the early formation of SiO_2 and P_2O_5 in the slag, the kinetics of decarburization slows down due to occupancy of these oxides at the interface of the metal drop, decreasing the effective surface area for carbon oxidation. In Cicutti's heat data, [4] which has been used for this modelling work, the initial lance height was kept at 2.5 m up to 4 min of the blow and after

that, it reduced to 2.2 m. It should be noted that with a decrease in 0.3 m height of the lance, the amount of droplets ejected can increase from 361 kg/s to more than 1000 kg/s. The increase in the amount of ejection of metal droplets into the emulsion can enhance the rate of refining. Thus, it appears that the sudden increase of the rate at blowing time of 4 min and 7 min are due to the result of a large number of droplets ejected into the emulsion. However, it was observed that at a constant lance position, the rate decreases after it reaches a peak value (between 6 to 7 min and 8 to 16 min). This behaviour is due to the decrease in the residence time of the metal droplets as a result of lowering in carbon concentration and FeO in the slag.

The present model calculation result shows that the peak value of decarburization occurs about 8 minutes after the start of blowing. This finding is consistent with the measured data of C concentration in the bath, which shows that the peak decarburization occurs between 6 to 11 minutes of the blowing time. Further, the total carbon removed by the emulsion has been computed by estimating the area under the curve of decarburization rate and blowing time. The calculation shows that 5200 kg of carbon has been removed by emulsion zone, which accounts for nearly about 76 pct of the total carbon refining during the entire blowing period. The slight increase in decarburization rate during the last stage of blowing (14 to 15 min) is due to increase in residence time of the droplets (0.8 mm drops as seen from the **Fig. 6**) as a result of slight over prediction of in FeO in the slag.

3.4. Decarburization in impact zone

The Eq. [13] has been applied to compute the decarburization rate from the impact zone at each numerical time step. **Figure 9** shows the decarburization rate predicted by the model in the jet impact zone. It was observed that the rate of carbon removal in the impact zone is primarily driven by a change in lance height in the blowing region when the carbon concentration in the bath is more than a critical value. In this region the carbon oxidation is controlled by oxygen diffusion into the melt, low lance height favours the kinetics of the reaction by creating a large

gas-metal interfacial area. The present model calculation shows that changing the lance height from 2.5 m to 1.8 m can improve the decarburization rate from 2.43 kg/s to 2.8 kg/s. Once the carbon reaches a threshold carbon concentration in the bath, the rate is limited by mass transport of carbon in the melt. In the present work, a fixed value of critical carbon concentration of 0.3 wt pct, has been used for the model calculation. The calculated decarburization rate is below 0.5 kg/s during this domain, and it is observed to decrease with a decrease in bath carbon concentration.

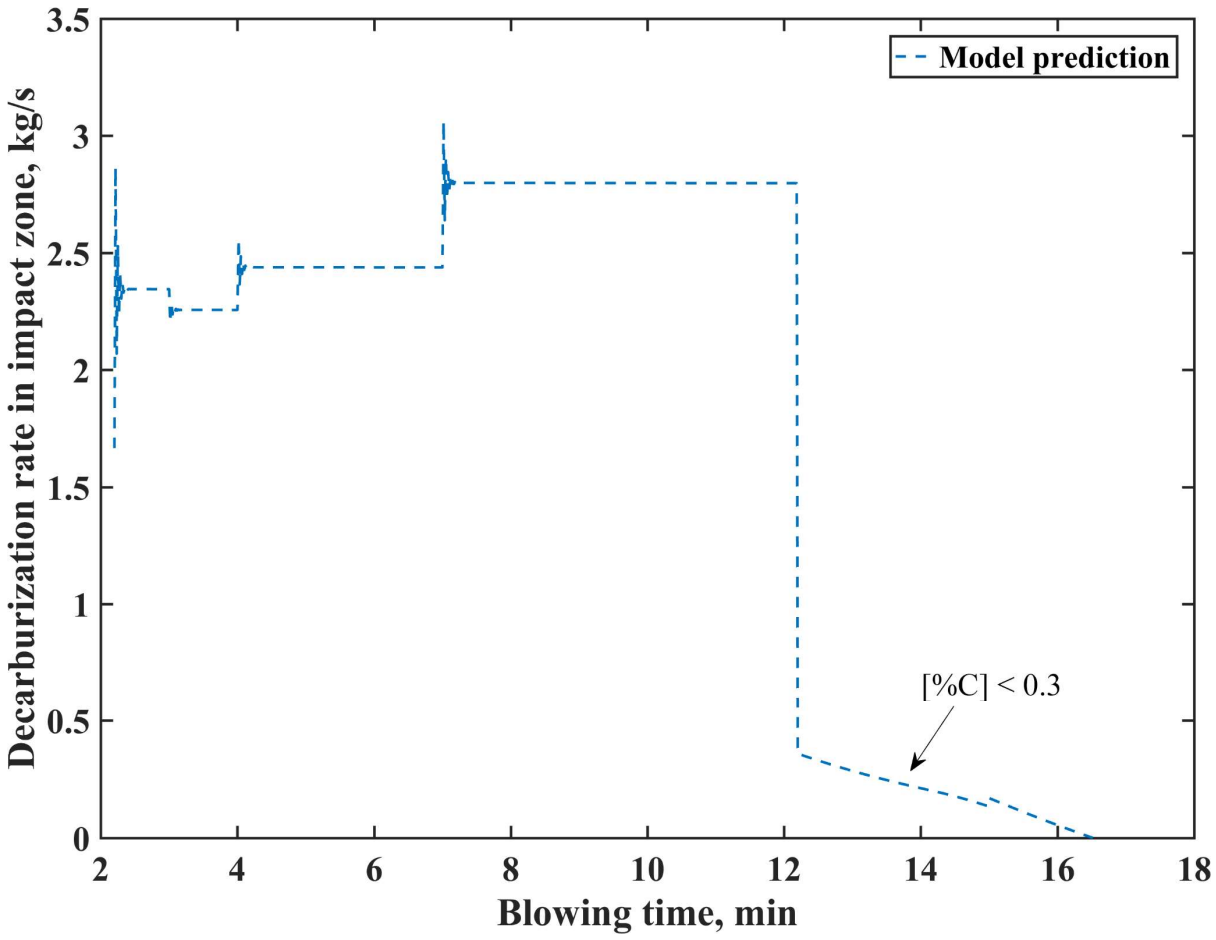

Figure 9: Model prediction of decarburization rate in impact zone

The area under the decarburization rate vs. blowing time profile was calculated by using trapezoid rule, and the total amount of carbon removed from the impact zone was estimated. The predicted result shows that approximately ~ 24 pct of C (total about 1607 kg) of total carbon has been withdrawn by the jet impact zone during the entire blowing period.

3.5. Overall decarburization in bath

The model prediction of carbon concentration in the bath as a function of blowing time is shown in **Fig. 10**. As can be seen from the figure, the model prediction agrees well with the industrially measured data of Cicutti *et al.*[4] The slow rate of decarburization reaction during the early part of the blowing process is well captured by the proposed surface limiting model. The three distinct regions can be observed from the model prediction of C in the bath, which is usually experienced in many decarburization profiles reported in the literature.

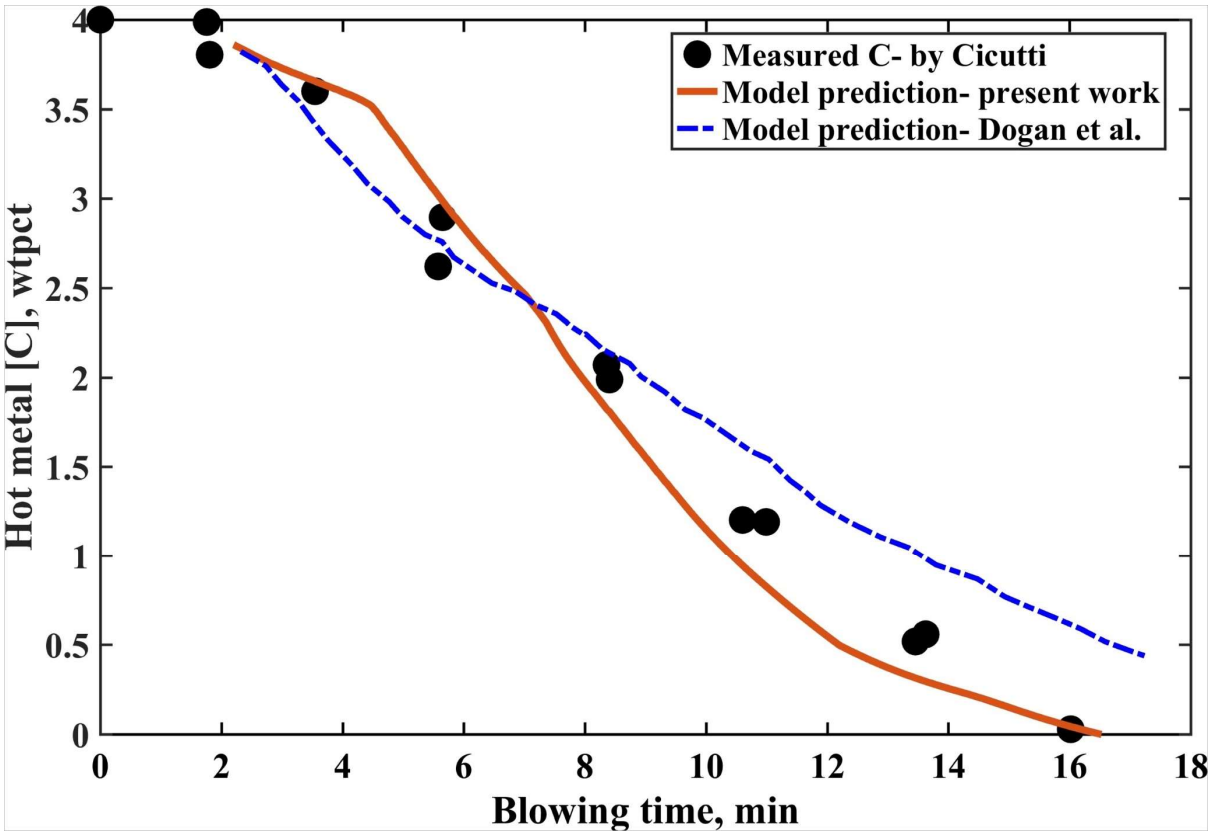

Figure 10: Model prediction of wt pct C in bath and its comparison with measured data

Region I: The rate of decarburization was observed to be weak during first 4.5 min of blowing time. The decarburization rate in this period is calculated to be 0.156 wt pct/min. The weak decarburization in this period is due to the ejection of a less number of droplets and the slow decarburisation kinetics of metal drops due to the presence of surface active oxides.

Region II: A constant rate of decarburization was observed between 4.5 to 12 min of blowing time. In this region, the lance height operates in the lowest position. That means a significant

number of drops goes into the emulsion phase. Further, the kinetic restriction due to reduction of interfacial area has been leveraged as the surface-active oxides start to dissolve in the slag and no longer form a barrier for the decarburization reaction at the interface. Thus, the rate of decarburization proceeds with full speed in this region. The rate is estimated to be approximately 0.25 wt pct/min. This value can be comparable with the peak decarburization of 0.3 wt pct /min reported by Cicutti *et al.*

Region III: The decarburization rate was further observed to decreases to a lower value after 12 min of the blow, once it reaches the critical carbon content in the bath. In this region, the rate of decarburization in the impact zone drastically decreases. However, some amount of refining by the emulsion zone was noticed for small sized droplets.

When compared with the previous model prediction by Dogan *et al.*,[8-10] the present model gives a better insight of carbon refining in a BOF, particularly during the initial and final part of the blow period. The slightly over-prediction of decarburization rate obtained from Dogan *et al.'s* model during the early part of the blow may be due to the model not taking the competitive kinetics of other elements such as Si and P in the melt, into account. Similarly, the weak decarburization rate predicted by Dogan's model during the blow end period is due to the low prediction of refining rate by emulsion zone. It was therefore evident that a single size of droplets cannot represent accurately the kinetics of reactions in the emulsion.

4. Conclusions

A multi-zone kinetic model has been established and used to simulate the decarburization rate of a top blowing steelmaking process. A significant improvement in the previous kinetic model developed by Dogan *et al.* was achieved by incorporating the adsorption effect of surface active oxides, the size distribution of initial droplets and modified droplet generation rate in the mathematical formulation in the emulsion zone of carbon refining. By combining this with the rate model for decarburization by the impact zone, the overall rate of carbon removal from the

bulk metal was simulated. The model predictions were validated with industrial data reported by Cicutti *et al.*[4], and an excellent agreement has been found. Based on the present study, the following conclusions can be drawn:

1. It was predicted that surface active oxides like SiO_2 and P_2O_5 in the slag are responsible for inhibiting the decarburization kinetics in emulsion particularly during the early blow period by blocking the interfacial sites for reaction. A classical surface coverage model can be suitable for studying decarburization kinetics in a multicomponent slag system.
2. The decarburization rate in the emulsion is predicted to be sensitive to the size of the droplet ejected from the melt. Not all the droplets ejected to the emulsion are participating in the reaction, only those drops which are able to bloat can only participate in effective emulsion-carbon conversion process. Present model calculation shows that only droplets having an initial diameter of less than 1.4 mm (1.4×10^{-3} m) are responsible for carbon refining by slag-metal emulsion.
3. The decarburization efficiency of a metal drop in emulsion is predicted to be depend on the initial size and carbon concentration. Generation of fine metal drops with higher carbon contents are predicted to be the favourable conditions for achieving high decarburisation in the emulsion phase..

Acknowledgement

The authors gratefully acknowledge Tata Steel, Netherlands for providing financial support for this work.

Nomenclature

a_i – thermodynamic activity (-)
A_{app}– Apparent area of the droplet (m^2)
C_b – Carbon concentration in bulk metal (wt pct)
C_{eq} – Equilibrium carbon concentration (wt pct)
D_c – Diffusion coefficient of carbon (m^2/s)
d- Diameter of droplet (m)

513 dW_C/dt – Decarburization rate (kg/s)
514 k_d – Mass transfer coefficient of decarburisation of a droplet (sec^{-1})
515 k_{eff} – Effective mass transfer coefficient with surface blocking effect (sec^{-1})
516 K_{SiO2} – Adsorption coefficient of SiO_2 (-)
517 K_{P2O5} – Adsorption coefficient of P_2O_5(-)
518 P_{amb}- Ambient pressure inside furnace (Pa)
519 p- Class in droplet size spectrum (-)
520 r_c – Decarburization rate of droplet (wt pct/s)
521 r_c^* – Critical decarburization for bloating (wt pct/s)
522 u – Velocity of droplet (m/s)
523 V_{app}– Apparent volume of the droplet (m^3)
524 W_b– Weight of bulk metal (kg)
525 Wc- Weight of carbon (kg)
526 W_{sc}- Weight of scrap added (kg)
527 W_m^{sl} – Weight of metal in slag (kg)
528 W_m^{eject} – Weight of metal ejected (kg)
529 W_m^{return} – Weight of metal return to the bath (kg)
530 W_{slag} – Weight of slag (kg)
531 W_{lime} – Weight of lime dissolute into slag (kg)
532
533 **Greek/Latin symbols**
534 θ_c –Fraction of occupied sites due to surface active oxides (-)
535 ρ_d – Density of droplet (kg/m^3)
536 $\rho_{d,0}$ – Initial density of droplet (kg/m^3)
537 σ – Surface tension (N/m)
538 Γ^0 – Saturation concentration of adsorbed species ($mole/cm^2$)
539 η –Efficiency of decarburization (-)
540
541 **Subscripts / superscripts**
542 em- Emulsion zone
543 iz- Impact zone
544 deC- Decarburisation
545
546 **References**
547 1. B. K. Rout, G. Brooks, M. A. Rhamdhani, Z. Li, F. Schrama, and J. Sun: *Metall. and Mater.*
548 *Trans. B*, 2018, pp : 1-21
549 2. P. Kozakevitch: *Journal of Metals* 1968, vol. 22, pp. 57-67.
550 3. H. W. Meyer, W. F. Porter, G. C. Smith and J. Szekely: *J METALS* 1968, vol. 20, pp. 35-42.
551 4. C. Cicutti, M. Valdez, T. Pérez, J. Petroni, A. Gómez, R. Donayo and L. Ferro: In *Sixth*
552 *International Conference on Molten Slags, Fluxes and Salts*, ed. ISS (Stockholm-Helsinki: Warrandale,
553 PA, 2000).
554 5. M. S. Millman, A. Kapilashrami, M. Bramming and D. Malmberg: European Union,
555 Luxembourg, 2011.
556 6. C. L. Molloseau and R. J. Fruehan: *Metal.l and Mater. Trans. B* 2002, vol. 33, pp. 335-44.
557 7. G. Brooks, Y. H. Pan, Subagyo and K. Coley: *Metallurgical and Materials Transactions B-Process*
558 *Metallurgy and Materials Processing Science* 2005, vol. 36, pp. 525-535.
559 8. N. Dogan, G. A. Brooks and M. A. Rhamdhani: *ISIJ Int.,* 2011, vol. 51, pp. 1086-92.
560 9. N. Dogan, G. A. Brooks and M. A. Rhamdhani: *ISIJ Int.,l* 2011, vol. 51, pp. 1093-1101.
561 10. N. Dogan, G. A. Brooks and M. A. Rhamdhani: *ISIJ Int.,* 2011, vol. 51, pp. 1102-1109.
562 11. R. Sarkar, P. Gupta, S. Basu and N. B. Ballal: *Metall. and Mater. Trans. B,* 2015, vol. 46, pp. 961-
563 976.

12. G. Brooks, Y. Pan, Subagyo and K. Coley: *Metall. and Mater. Trans. B,*2005, vol. 36, pp. 525-35.
13. Subagyo, G. A. Brooks, K. S. Coley and G. A. Irons: *ISIJ Int.,* 2003, vol. 43, pp. 983-989.
14. B. K. Rout, G. A. Brooks, M. A. Rhamdhani and Z Li: *Metall. and Mater. Trans. B*,2016, vol 47, No. 6. Pp. 3350-61.
15. S. C. Koria and K. W. Lange: *Metall. Trans. B* 1984, vol. 15, pp. 109-16.
16. Q. L. He and N. Standish: *ISIJ Int.,* 1990, vol. 30, pp. 305-09.
17. H. Sun: *ISIJ Int.,*2006, vol. 46, pp. 1560-69.
18. E. Chen and K. S. Coley: *Ironmak. & Steelmak.* 2010, vol. 37, pp. 541-45.
19. E. W. Mulholland, G. S. F Hazeldea and M. W. Davies: *J Iron Steel,* 1973, vol. 211, pp. 632-39.
20. D. E. Woolley and U. B. Pal: In *58 th Ironmaking Conference*, (1999), pp 413-29.
21. W. M. Kim, G. Granzdorffer and H. Fine: *Steel Res.* 1988, vol. 60, pp. 166-70.
22. W. Pan, M. Sano, M. Hirasawa and K. Mori: *ISIJ Int.* 1991, vol. 31, pp. 358-65.
23. R. D. Morales, H. Rodríguez-Hernández, P. Garnica-González and J. A. Romero-Serrano: *ISIJ Int.,* 1997, vol. 37, pp. 1072-80.
24. D. J. Price and M. J. Jones: In *Process Engineering of Pyrometallurgy Symposium*, (1974).
25. G. A. Brooks, M. A. Rhamdhani, K. S. Coley, Subagyo and Y. Pan: *Metall. and Mater. Trans. B* 2008, vol. 40, pp. 353-62.
26. Y. Chung and A. Cramb: *Metall. and Mater. Trans B,* 2000, vol. 31, pp. 957–71.
27. X. Hu, H. Matsuura and F. Tsukihashi: *Metall. and Mater. Trans. B* 2006, vol. 37, pp. 395-401.
28. K. Chou, U. B. Pal and R. G. Reddy: *ISIJ Int.,* 1993, vol. 33, pp. 862-68.
29. ET Turkdogan: *Fundamentals of steelmaking*. (The Institute of Materials, London, 1996), pp. 182.
30. S. Kitamura, T. Kitamura, K. Shibata, Y. Mizukami, S. Mukawa and J. Nakagawa: *ISIJ Int.,* 1991, vol. 31, pp. 1322-28.
31. Honglei Sun and Guangqing Zhang: In *ICS proceeding*, (2005), pp 257-68.
32. F. D. Richardson: *Physical chemistry of melts in metallurgy*. Academic Press (Elsevier), vol. 2, 1974, p. 441 .

Appendix I

Calculation of adsorption coefficient K_{SiO2}

Combining Gibbs isotherm with that of Langmuir, the surface tension of FeO-SiO_2 slag system can be expressed by the following equation:

$$\sigma = \sigma_0 - RT\Gamma^0_{SiO_2} \ln(1 + K_{SiO_2} a_{SiO_2}) \quad \text{(A1)}$$

Where $\Gamma^0_{SiO_2}$ is the saturation concentration of adsorbed SiO_2, K_{SiO2} is the adsorption equilibrium constant and a_{SiO2} is the activity of SiO_2. σ is the surface tensions of the FeO-SiO2 melt and σ_0 is the surface tension of SiO_2 free iron oxide melt. The above equation can be rearranged in the form of a linear equation as $y = mx$ where $y = \exp\left(\frac{\sigma_0 - \sigma}{RT\Gamma^0_{SiO_2}}\right) - 1$ and $x =$

a_{Si} $_2$. The plot of y vs x is shown in **Fig. A1**. The saturation concentration $\Gamma^0_{SiO_2}$ was taken to be6.55 × 10^{-10} mole/cm^2 from the surface tension data by Richardson *et al.*[32] The value of K_{SiO2} was calculated to be 8.86from the slope of the plot in Fig. A1. Similar value of adsorption coefficient of SiO_2 was reported by Wei *et al.*[22] for FeO-SiO_2 slag system.

Calculation of adsorption coefficient K_{P2O5}

The slag containing P_2O_5 can interfere with the FeO adsorption on the slag-metal interface and thus can retard the decarburization rate. Hu *et al.* [27] reported that the for FeO_x-P_2O_5 melts, the activity of P_2O_5 follow Henry's law when the concentration of P_2O_5 falls below 8-mole pct. The fraction of occupied sites of P_2O_5 at the interface according to Hu *et al.* [27]is defined as:

$$\theta_p = \frac{0.65(mole\ pct\ P_2O_5\ )}{1 + 0.65(mole\ pct\ P_2O_5)} \quad \text{(A2)}$$

From Eq. A2, the value of $K_{P_2O_5}a_{P_2O_5}$ is assumed to be $0.65(mole\ pct\ P_2O_5)$ in the present work.

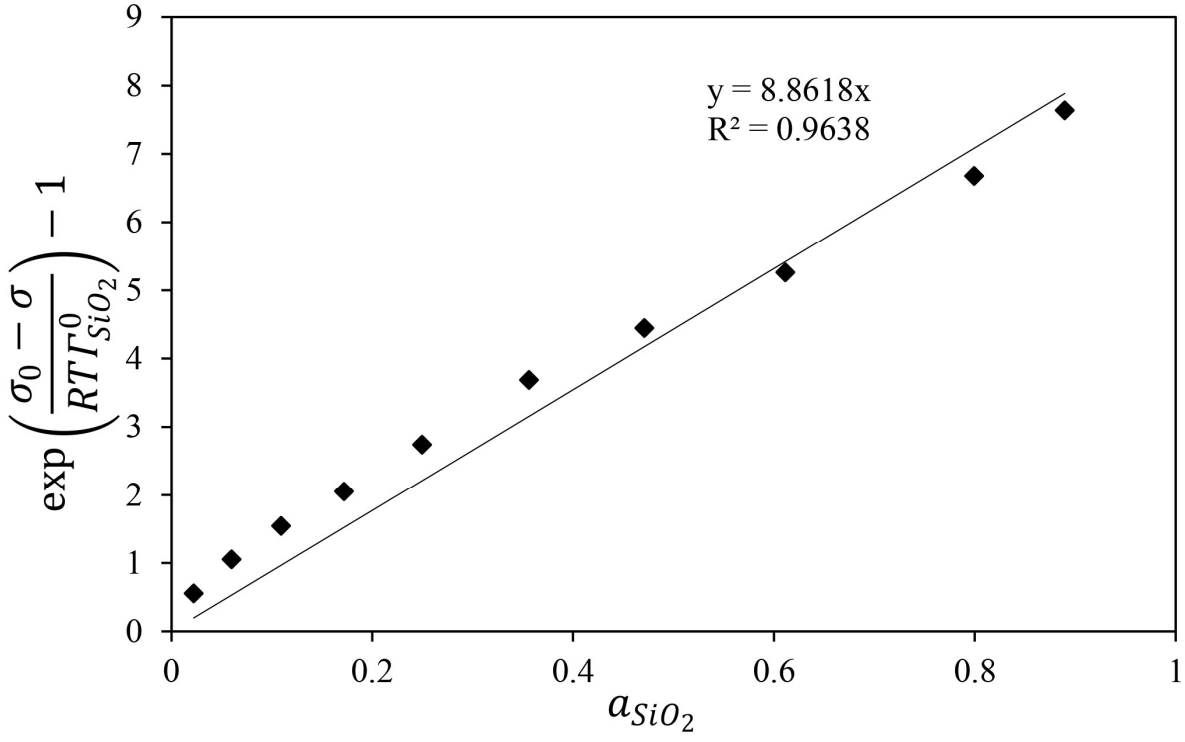

Figure A1: Calculation of K_{SiO2} from surface tension data

Effect of S on decarburization rate

Several studies indicated that the presence of S in the iron droplet influences the rate of decarburization by FeO in the slag. Sulphur is a highly surface active element in liquid iron and it can affect the decarburization rate in two ways: (i) segregates at the interface and limits the interfacial area by blocking the reaction sites (ii) decrease the slag-metal interfacial tension and makes it easier for emulsification (enhances the interfacial area). Since the rate of reaction is directly proportional to the reaction area, the competition between the positive effect of emulsion formation and negative effect of surface blockage has been observed. Molloseau *et al.* [6] observed that decarburization reaches a maximum value when S = 0.011 wt pct and further increase in S decreases the reaction rate. Similar observation was made by Chen *et al.* [18] and this value has been reported to be 0.013 wt pct. The total interfacial area evolution for Fe-C- S droplets in slag is a combination of both bloating due to CO nucleation and emulsification due to the presence of S.

$$Total\ interfacial\ area = A_{bloating}(CO) + A_{emulsfication}(S) \quad \text{(A3)}$$

Modelling of interfacial reaction area due to the effect of S in the iron droplet is complex. The decrease in surface area due to adsorption of S at the interface can be described by using surface blockage mechanism. However, it is difficult to distinguish between the surface area change due to CO nucleation and emulsification by surface active elements such as S. In the model proposed by Brooks *et al.*[12], the total change in interfacial area of the metal droplet has been empirically correlated with decarburization rate and slag FeO. The correlation was developed on the basis of Fe-C-0.011S data, where the rate of decarburization is observed to be at peak value. This method of calculation of interfacial area can be considered as standard state and for high concentration of sulphur (S > 0.011 wt pct) decarburization rate can be calculated by the correcting the interfacial area with respect to the standard state. For application of Brooks *et al.*'s model for high S concentration, we defined a rate constant modifying as

$$\varphi = \frac{rate\ of decarburization}{Maximum\ rate\ of\ decarburization\ observed\ at\ S = 0.011\ wt\ pct} \quad \text{(A4)}$$

φ = 1 means the rate of decarburization reaches the maximum value due to large increase in surface area caused by S. At higher S level φ is less than 1 due to the surface blocking effect of S on reaction interface.

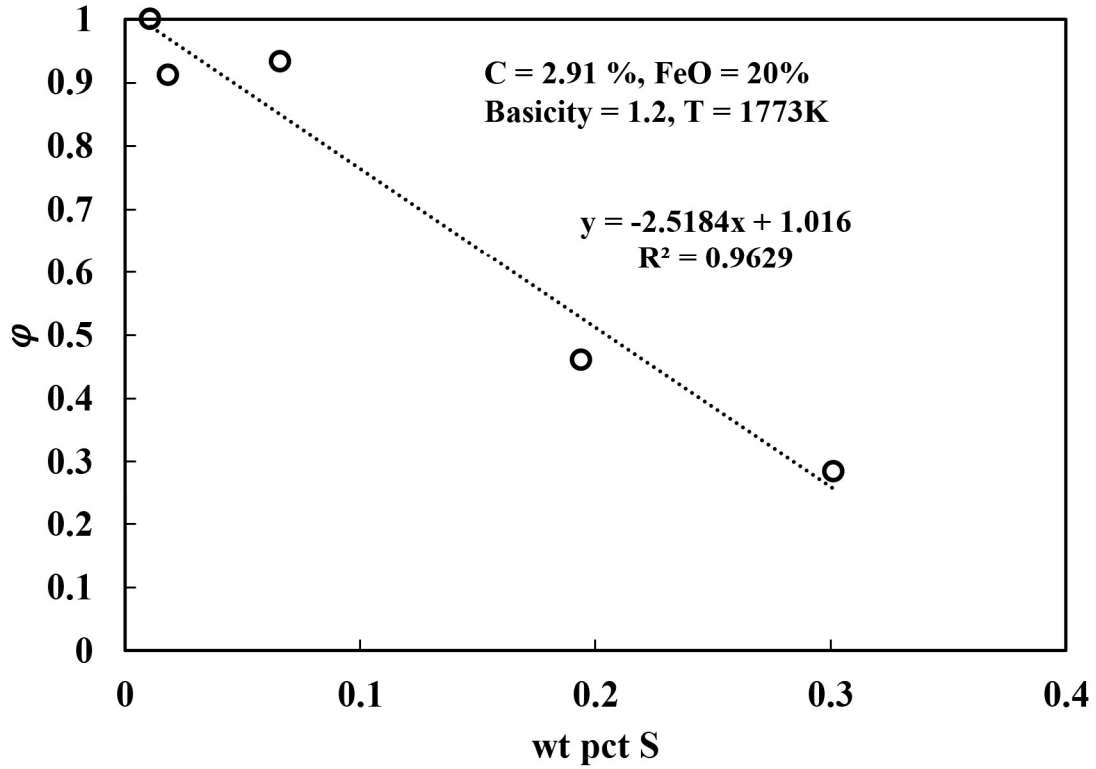

Figure A2: Rate constant modifying parameter as a function of S in the metal droplet (Data adopted from Molloseau *et al*.[6] and Chen *et al*.[18])

At high S level in the steel, the decarburization rate must be multiplied by the rate constant modified parameter to get the actual rate due to the effect of sulphur. The experimental data by Molloseau *et al.* and Chen *et al.* have been used and φ as a function of S in the droplet is plotted in **Fig. A2.**

For S > 0.011 and S < 0.3 wt pct

$$\varphi = 1.016 - 2.5184 \times [wt\ pct\ S] \quad \text{(A5)}$$

$$k_{eff}^{s} = k_{eff} \times \varphi \quad \text{(A6)}$$

650

651 It should be noted that due to lack of experimental data, the empirical equation derived for $\boldsymbol{\varphi}$
652 is simplistic in nature and it has been derived at constant C, slag FeO and temperature. In
653 Cicutti's heat data used for the present model calculation, S concentration is about 0.015 wt
654 pct. The modifying rate parameter φ corresponds to this S level estimated to be 0.96 in the
655 present work.

656 **Activity coefficient of C**
657
658 The activity coefficient of C was calculated by the following relationship[28]:

$$a_C = [\%C]\, f_c \quad \text{(A7)}$$

$$\log f_c = 0.1666[\%C] - 0.01585[\%C]^2 + 9.9613 \times 10^{-7}[\%C]^3(T-273) + 3.0246 \times 10^{-5}[\%C](T-273) \quad \text{(A8)}$$

659
660
661
662 **Caption list**
663 **Figure captions:**
664 Figure 1: Dogan et al.'s model prediction of bath [wt pct C] refined by emulsion zone on the
665 basis of different droplet generation rates

666 Figure 2: Algorithm for overall decarburization rate estimated from two reaction zones

667 Figure 3: Estimation of mass transfer coefficient of C for Fe-C-S droplet

668 Figure 4: Modelling of decarburization kinetics of Fe-C-Si droplets in slag

669 Figure 5: Decarburization efficiency of a metal droplet as a function of droplet size

670 Figure 6: Residence time prediction of the metal droplets in slag as a function of blowing
671 time

672 Figure 7: Qualitative representation of the mechanism of bloating of metal drops in slag

673 Figure 8: Decarburization rate by emulsion calculated by the model

674 Figure 9: Model prediction of decarburization rate in impact zone

675 Figure 10: Model prediction of C wt pct in bath and comparison with measured data

676 Figure A1: Calculation of K_{SiO2} from surface tension data

677 Figure A2**:** Rate constant modifying parameter as a function of S in the metal droplet (Data

678 adopted from Molloseau *et al.*[6] and Chen *et al.*[18])

679
680
681 **List of Tables:**
682 Table 1: Different aspects of modeling of various parameters relevant to kinetics of

683 decarburization in slag-metal emulsion (NC: not considered, C: considered)

Authors	Residence time	Kinetics (single drop)	Droplet generation rate	Size distribution	Effect of other elements	Effect of slag	Overall kinetics emulsion
Koria *et al.*, [15]Subagyo *et al.* [13]	NC	NC	NC	C	NC	NC	NC
Subagyo *et al.*, [13]He *et al.*,[16] Rout *et al.*[14]	NC	NC	C	NC	NC	NC	NC
Brooks *et al.*[7]	C	C	NC	NC	NC	NC	NC
Sun H.[17]	C	C	NC	NC	C	NC	NC
Chen and Coley[18]		C					
Dogan *et al.*[8-10]	C	C	C	NC	NC	NC	C

Sarkar *et al.*[11]	C	C	C	NC	C	NC	C

684